

# ISAC FROM THE SKY: NET-ZERO ENERGY UAV TRAJECTORY DESIGN

Xiaoye Jing<sup>1</sup>, Fan Liu<sup>2</sup>, Christos Masouros<sup>1</sup>

<sup>1</sup>University College London, London WC1E 7JE, UK

<sup>2</sup>Southern University of Science and Technology, Shenzhen 518055, China

## ABSTRACT

Unmanned aerial vehicle (UAV) can work as a portable base station providing not only the communication service to ground users, but also the sensing functionality to localize targets of interests. In this paper, we consider a scenario with one rotary-wing UAV to transmit signals for a communication service and receive echos for a target estimation. We propose a multi-stage trajectory design method to jointly improve both the communication and sensing (C&S) performances. We formulate the trajectory design problem into a weighted optimization problem and propose an iterative algorithm to solve it. Numerical results show the performance trade-off between C&S.

*Index Terms*— Cramér-Rao bound, joint sensing and communication, convex optimization

## 1. INTRODUCTION

Designing communication and sensing (C&S) systems in a joint manner so that they can share the common hardware and signals, is envisioned as a promising solution to reduce hardware cost and improve spectral efficiency, which has motivated the recent research interest in integrated sensing and communication (ISAC) technology [1–3]. ISAC has been widely studied for numerous wireless applications, such as Wi-Fi based indoor localization and cooperative C&S in unmanned aerial vehicle (UAV) networks [4]. In particular, different from the conventional terrestrial cellular networks, UAV is an off-the-grid network solution, becoming indispensable to realize net-zero energy operation in the next generation of wireless network [5]. UAV based communication systems and UAV based sensing systems are regarded as important components for non-terrestrial wireless networks. Applying ISAC technology into UAV networks is a possible solution to minimize the payload of UAVs, enabling the hardware reuse between C&S [6].

There are some existing UAV researches based on ISAC. In [4], a power allocation scheme was proposed in a static multi-UAV network to maximize a utility performance. The UAV deployment was determined via a clustering approach and a power allocation scheme was studied based on target locations. To fully exploit the UAV mobility for C&S

performance improvement, ISAC technology with moving UAVs were proposed. In [7], a periodic ISAC framework where sensing is periodically performed with continuous communication was proposed. The authors maximized the communication performance by optimizing the sensing instant, UAV trajectory and beamforming. In [8], the authors considered a scenario where one UAV sends communication signals to multiple users and senses potential targets at interested areas. The objective was to maximize the throughput of communication users by jointly optimizing UAV locations and transmit beamforming. Although the beampattern gain optimized in [7] and [8] above is a valid performance metric for sensing, it fails to reflect the specific target estimation error. This motivates the study in our work focusing on the Cramér-Rao Bound (CRB) which provides a lower bound for mean squared estimation error, thus, directly reflects the estimation error of target coordinates [4].

In this paper, we consider the ISAC based UAV trajectory design problem with one moving UAV, which aims to realize the performance trade-off between C&S. The objective is to jointly minimize the CRB for target estimation and maximize the downlink rate for user communication. By considering the limited capacity of UAV on-board battery, we impose an energy constraint when designing the UAV flying trajectory. To improve the accuracy of UAV trajectory design, we propose a multi-stage design approach to update target estimate frequently.

## 2. SYSTEM MODEL AND TRAJECTORY PROTOCOL

We consider a rectangular system area with a dimension  $L_x$  by  $L_y$  and UAV departures from one charging base at  $[x_B, y_B]^T$ . As shown in Fig.1, system includes one rotary-wing UAV, one communication user and one target. The UAV broadcasts signals embedded data to the ground during its flight. The user can receive signals continuously. Meanwhile, the flight trajectory includes hovering points. At each point, UAV receives one echo which is from the signal transmitted by itself at the same point and then reflected by the target. The propagation delay between signal and echo is obtained, based on which the distance between the hovering point and the target is measured. Finally, these distance measurements

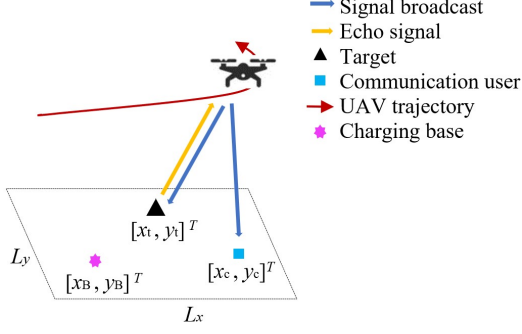


Fig. 1. Proposed system.

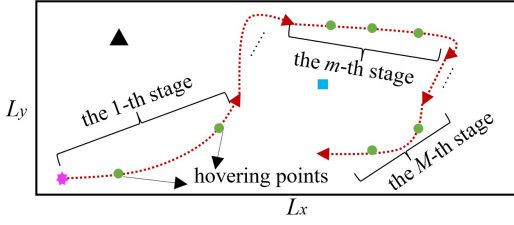


Fig. 2. Multi-stage approach.

from various points can be fused together to obtain the horizontal coordinates of the target via estimation method, e.g., maximum likelihood estimation (MLE).

The communication user's location is  $[x_c, y_c]^T$ , known *a priori* via Global Navigation Satellite System. The UAV trajectory is decided by the distribution of the user and target. The ground-truth location of the target, denoted by  $[x_t, y_t]^T$  is initially unknown. In this case, trajectory design should be dependent on an estimate of  $[x_t, y_t]^T$ , which is denoted as  $[\hat{x}_t, \hat{y}_t]^T$ . Note that there may exist a gap between  $[\hat{x}_t, \hat{y}_t]^T$  and  $[x_t, y_t]^T$ , leading to an accuracy loss in the designed trajectory. In order to obtain a more accurate trajectory, we propose a multi-stage design approach in Fig. 2.

Before UAV departure, we obtain a coarse target estimate  $[\hat{x}_t^0, \hat{y}_t^0]^T$ . UAV trajectory decided in the 1-th stage is based on  $[x_c, y_c]^T$  and  $[\hat{x}_t^0, \hat{y}_t^0]^T$ . The UAV starts its flight and follows the obtained trajectory to transmit signals. After it completes the 1-th stage flight, we estimate an updated location,  $[\hat{x}_t^1, \hat{y}_t^1]^T$ . Now, the trajectory design comes into the 2-th stage, which is based on  $[x_c, y_c]^T$  and  $[\hat{x}_t^1, \hat{y}_t^1]^T$ . Then, the UAV starts its flight for the 2-th stage from the final waypoint of the 1-th stage. We set  $m$  as the stage index and UAV trajectory in the  $m$ -th stage is described by  $N_m$  2-dimensional waypoints,  $\mathbf{s}_n^m \in \mathbb{R}^{2 \times 1}$  ( $n = 1, \dots, N_m$ ). We concatenate these waypoints in a matrix  $\mathbf{S}_m = [\mathbf{s}_1^m, \dots, \mathbf{s}_{N_m}^m] \in \mathbb{R}^{2 \times N_m}$  for later use. The updated estimate of  $[x_t, y_t]^T$  after UAV completes the  $m$ -th stage is denoted as  $[\hat{x}_t^m, \hat{y}_t^m]^T$ .

We set  $N_m$  is same in each stage and pre-determined as  $N_{\text{stg}}$ . We notice that the UAV flight duration and distance are

uncertain and dependent on its available battery capacity, so that after each stage, we calculate the UAV's remaining battery capacity. If current capacity is not enough to support a flight with  $N_{\text{stg}}$  waypoints, we denote the next stage as the final stage by index  $M$  and calculate the maximum number of waypoints in the  $M$ -th stage as  $N_M = N_{\text{lst}}$ . There are  $K_m$  hovering points included in the  $m$ -th stage to perform sensing. Specifically, after the UAV flies over  $\mu - 1$  waypoints ( $\mu$  is a given integer), it hovers at the next waypoint with a duration  $T_h$  to receive an echo, so that  $K_m = \text{floor}\left(\frac{N_m}{\mu}\right)$ . The  $k$ -th hovering point in the  $m$ -th stage is

$$[x_k^m, y_k^m]^T = \mathbf{s}_{\mu k}^m, k = 1, 2, \dots, K_m. \quad (1)$$

Hovering points in the  $m$ -th stage are denoted by vectors  $\mathbf{x}_m = [x_1^m, \dots, x_{K_m}^m]^T$  and  $\mathbf{y}_m = [y_1^m, \dots, y_{K_m}^m]^T$  for later use. Velocity between consecutive waypoints is

$$\mathbf{v}_n^m = \frac{\mathbf{s}_n^m - \mathbf{s}_{n-1}^m}{T_f}, n = 2, \dots, N_m, \quad (2)$$

$$\mathbf{v}_1^m = \frac{\mathbf{s}_1^m - \mathbf{s}_{N_{m-1}}^{m-1}}{T_f}, n = 1. \quad (3)$$

$T_f$  is the duration between waypoints and we use  $\mathbf{V}_m = [\mathbf{v}_1^m, \dots, \mathbf{v}_{N_m}^m]$  for later use.

### 3. PROBLEM FORMULATION

The propagation channel is dominated by the light-of-sight (LoS) link [9]. For communication, the channel power gain from the UAV at the  $n$ -th waypoint in the  $m$ -th stage to the communication user can be expressed as

$$h_n^m = \frac{\alpha_0}{[d_{m,n}^c]^2}, \quad (4)$$

where  $\alpha_0$  is the channel power at the reference distance  $d_{m,n}^c = 1\text{m}$  [10].  $d_{m,n}^c = \sqrt{H^2 + \|\mathbf{s}_n^m - [x_c, y_c]^T\|^2}$  denotes the distance from the waypoint to the user.  $H$  is the UAV altitude. We use the average communication rate as the performance metric. The average rate from the 1-th to the  $m$ -th stage can be expressed as

$$\bar{R}_m = \frac{1}{\sum_{i=1}^m N_i} \sum_{i=1}^m \sum_{n=1}^{N_i} B \log_2 \left( 1 + \frac{P h_n^m}{\sigma_0^2} \right). \quad (5)$$

where  $P$  is the transmit power.  $\sigma_0^2$  is the noise power at the receiver.  $B$  is the channel bandwidth.

In sensing model,  $[x_t, y_t]^T$  is determined by at least 3 different distances. We denote  $\tau_n^m$  as the two-way propagation delay of the signal from  $[x_k^m, y_k^m]^T$  to the target and reflected back to  $[x_k^m, y_k^m]^T$ .  $d_{m,k}^s = \frac{1}{2} c \tau_k^m$  is the distance from the UAV to the target and its measurement is

$$\hat{d}_{m,k}^s = d_{m,k}^s + w_k^m, \quad (6)$$

where  $c$  is the speed of light.  $w_k^m \sim \mathcal{N}\left(0, [\sigma_k^m]^2\right)$  is subject to individual Gaussian distribution [11] and

$$[\sigma_k^m]^2 = \frac{a\sigma_0^2 [d_{m,k}^s]^4}{PG_p\beta_0}, \quad (7)$$

where  $a$  is a pre-determined constant related to the system setting.  $G_p$  is the signal processing gain.  $\beta_0$  is the channel power at the reference distance  $d_{m,k}^s = 1\text{m}$  [10].

To assess the estimation performance, we calculate CRBs of  $x_t$  and  $y_t$ . From [12] and [13] (eq. 3.31), CRBs of  $x_t$  and  $y_t$  in the  $m$ -th stage are expressed as

$$\text{CRB}_m^{x_t} + \text{CRB}_m^{y_t} = \frac{\Theta_m^b}{\Theta_m^a \Theta_m^b - [\Theta_m^c]^2} + \frac{\Theta_m^a}{\Theta_m^a \Theta_m^b - [\Theta_m^c]^2}, \quad (8)$$

$$\Theta_m^a = \sum_{i=1}^m \sum_{k=1}^{K_i} \frac{(x_k^m - \hat{x}_t^{m-1})^2}{[\sigma_k^m]^2 [d_{m,k}^s]^2} + \frac{8(x_k^m - \hat{x}_t^{m-1})^2}{[\sigma_k^m]^2}, \quad (9)$$

$$\Theta_m^b = \sum_{i=1}^m \sum_{k=1}^{K_i} \frac{(y_k^m - \hat{y}_t^{m-1})^2}{[\sigma_k^m]^2 [d_{m,k}^s]^2} + \frac{8(y_k^m - \hat{y}_t^{m-1})^2}{[\sigma_k^m]^2}, \quad (10)$$

$$\Theta_m^c = \sum_{i=1}^m \sum_{k=1}^{K_i} \frac{(x_k^m - \hat{x}_t^{m-1})(y_k^m - \hat{y}_t^{m-1})}{[\sigma_k^m]^2 [d_{m,k}^s]^2} \quad (11)$$

$$+ \sum_{i=1}^m \sum_{k=1}^{K_i} \frac{8(x_k^m - \hat{x}_t^{m-1})(y_k^m - \hat{y}_t^{m-1})}{[\sigma_k^m]^2}, \quad (12)$$

Finally, the trajectory design problem in the  $m$ -th stage is formulated to jointly increase data rate and decrease CRB as

$$\text{P1}(m) : \min_{\substack{\mathbf{s}_m, \mathbf{x}_m, \\ \mathbf{y}_m, \mathbf{v}_m}} \eta (\text{CRB}_m^{x_t} + \text{CRB}_m^{y_t}) - (1 - \eta) \bar{R}_m$$

$$\text{s.t. } \|\mathbf{v}_n^m\| \leq V_{\text{up}}, n = 1, \dots, N_m, \quad (13)$$

$$T_f \sum_{n=1}^{N_m} P(\|\mathbf{v}_n^m\|) + T_h K_m P(0) \leq E_m. \quad (14)$$

The weighting factor  $\eta$  takes values between 0 and 1, and higher  $\eta$  means that the trajectory design assigns higher priority on sensing.  $V_{\text{up}}$  is the maximum UAV speed.  $E_m$  is the UAV remaining battery capacity after the  $m - 1$ -th stage. The left-hand-side (LHS) of (14) is the energy consumption expression found in [10]. We denote the objective function as  $\Phi_m$  for later use.

#### 4. PROPOSED ALGORITHM

In this section, an iterative algorithm is proposed for solving P1( $m$ ). Firstly, the non-convex constraint (14) can be addressed with successive convex approximation (SCA). More

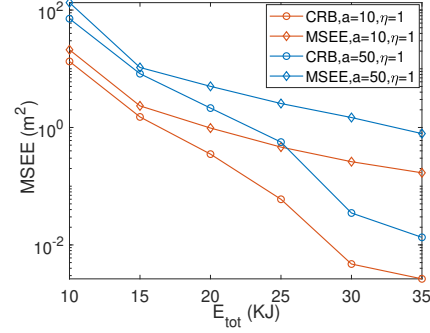


**Fig. 3.** Sensing performance with different  $a$  ( $N_{\text{stg}} = 25$ ).

details can be found in [10]. We use the upper bound, which is convex to substitute the LHS of (14) in each iteration.

Secondly, we tackle the non-convexity of  $\Phi_m$ . To proceed with SCA algorithm, at the  $l$ -th iteration, let us approximate  $\Phi_m$  by its first-order Taylor expansion near given points from the  $l - 1$ -th iteration as

$$\begin{aligned} \Phi_m^l &\approx \Phi_m^{l-1} + \sum_{k=1}^{K_m} \left\{ \nabla \Phi_{[x_k^m]^{l-1}} \left( x_k^m - [x_k^m]^{l-1} \right) \right\} \\ &+ \sum_{k=1}^{K_m} \left\{ \nabla \Phi_{[y_k^m]^{l-1}} \left( y_k^m - [y_k^m]^{l-1} \right) \right\} \\ &+ \sum_{n=1}^{N_m} \left\{ \nabla \Phi_{[\mathbf{s}_n^m(1)]^{l-1}} \left( \mathbf{s}_n^m(1) - [\mathbf{s}_n^m(1)]^{l-1} \right) \right\} \\ &+ \sum_{n=1}^{N_m} \left\{ \nabla \Phi_{[\mathbf{s}_n^m(2)]^{l-1}} \left( \mathbf{s}_n^m(2) - [\mathbf{s}_n^m(2)]^{l-1} \right) \right\}. \quad (15) \end{aligned}$$

where  $\nabla \Phi_{[x_k^m]^{l-1}}$ ,  $\nabla \Phi_{[y_k^m]^{l-1}}$ ,  $\nabla \Phi_{[\mathbf{s}_n^m(1)]^{l-1}}$  and  $\nabla \Phi_{[\mathbf{s}_n^m(2)]^{l-1}}$  represent the gradient of  $\Phi_m$  with respect to  $x_k^m$ ,  $y_k^m$ ,  $\mathbf{s}_n^m(1)$  and  $\mathbf{s}_n^m(2)$  from the  $l - 1$ -th iteration respectively.

By substituting  $\Phi_m$  with (15) and solving P1( $m$ ), we can reach to optimal solutions as  $[x_k^m]^*$ ,  $[y_k^m]^*$  and  $[\mathbf{s}_n^m]^*$ . Since this is a minimization problem, in the  $l$ -th iteration,  $[x_k^m]^* - [x_k^m]^{l-1}$ ,  $[y_k^m]^* - [y_k^m]^{l-1}$  and  $[\mathbf{s}_n^m]^* - [\mathbf{s}_n^m]^{l-1}$  yields descent directions [14]. Next, we move along the descent direction with a stepsize  $\omega_m \in [0, 1]$  to find updated points as

$$[x_k^m]^l = [x_k^m]^{l-1} + \omega_m \left( [x_k^m]^* - [x_k^m]^{l-1} \right), \quad (16)$$

$$[y_k^m]^l = [y_k^m]^{l-1} + \omega_m \left( [y_k^m]^* - [y_k^m]^{l-1} \right), \quad (17)$$

$$[\mathbf{s}_n^m]^l = [\mathbf{s}_n^m]^{l-1} + \omega_m \left( [\mathbf{s}_n^m]^* - [\mathbf{s}_n^m]^{l-1} \right), \quad (18)$$

$$k = 1, \dots, K_m, n = 1, \dots, N_m. \quad (19)$$

#### 5. NUMERICAL RESULTS

This section provides numerical results to evaluate the performance trade-off of C&S. We set  $[x_B, y_B]^T = [100\text{m}, 100\text{m}]^T$ .

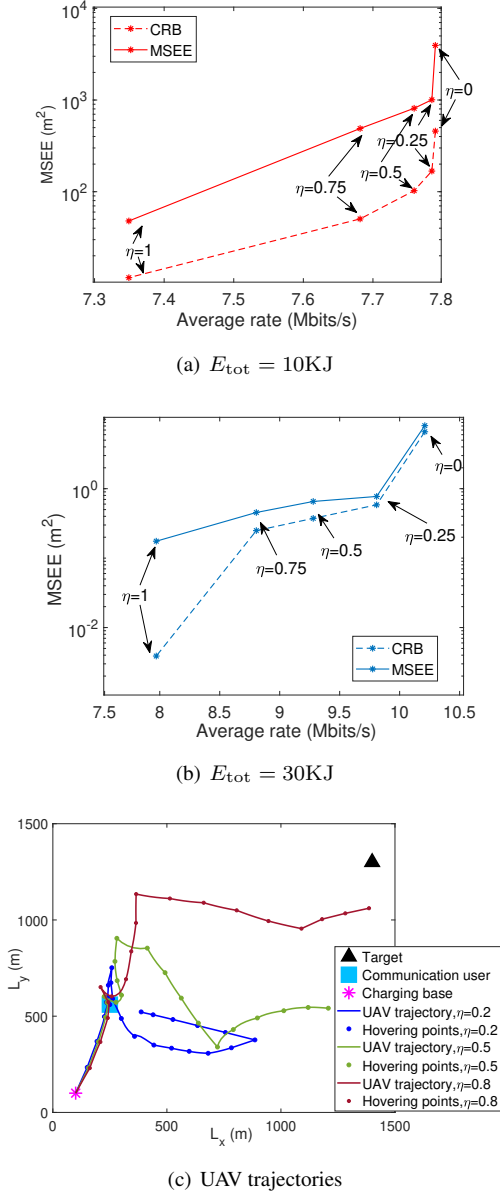


**Fig. 4.** Trade-off between C&S ( $N_{\text{stg}} = 25$ ).

$E_{\text{tot}}$  is the UAV battery capacity before its departure. The location of the target and the communication user are generated in simulation based on a uniform point distribution. Term “MSEE” denotes the real mean squared estimation error of  $x_t$  plus of  $y_t$ . Simulation parameters are shown in Table I.

In Fig. 3,  $\eta = 1$  means the trajectory design only consider sensing, so that we can evaluate the sensing performance with different measurement noise  $a$ . We use “CRB” to represent  $\text{CRB}_M^{x_t} + \text{CRB}_M^{y_t}$  after UAV completes its final stage. It is shown that, compared with  $a = 10$ , both the real estimation error and the CRB increase when  $a = 50$ , since when  $a$  has a larger value, the sensing performance becomes worse. We

**Table 1.** Simulation parameters

parameter	value	parameter	value
$\alpha_0$	-50 dB	$\beta_0$	-47 dB
$N_0$	-170 dBm/Hz	$\sigma_0^2$	$N_0 B$
P	20 dBm	B	1 MHz
$G_p$	$0.1B$	$V_{\text{up}}$	30 m/s
H	200 m	$T_h$	1 s
$T_f$	1.5 s	$\mu$	5
$L_x$	1500 m	$L_y$	1500 m

also observe that as  $E_{\text{tot}}$  increases, both estimation error and CRB decrease, that is because the UAV can fly longer distance and be closer to the target with larger  $E_{\text{tot}}$  to get more distance measurements with higher accuracy.

In Fig. 4, we aim to show C&S trade-off by tuning the weighting factor  $\eta$ . It can be seen that there exists a trade-off between the average communication rate and estimation error, especially with lower  $E_{\text{tot}}$ . The estimation error changes smoothly from  $\eta = 0.25$  to  $\eta = 1$ , but sharply from  $\eta = 0$  to  $\eta = 0.25$ , meaning that as long as the sensing is considered in designing trajectory, even if  $\eta$  is small, the sensing performance can result in a huge enhancement with a slight decrease on communication performance. We can also observe from Fig. 4 (a) and (b) that when UAV has higher  $E_{\text{tot}}$ , both C&S have better performance. Fig. 4 (c) shows the UAV trajectories with different  $\eta$  to explicate this trade-off. It can be observed that with a larger  $\eta$ , the UAV trajectory is more suitable for performing sensing. Specifically, the UAV flies closer to the target, and the angle distribution between the target and hovering points is more diverse, so that the sensing can be from more directions, resulting in a better estimation.

## 6. CONCLUSION

In this paper, we have considered the UAV trajectory design problem in an ISAC based UAV system. A multi-stage approach has been proposed to update target estimate. We formulated a weighted optimization problem for the trajectory design to achieve a flexible performance trade-off between C&S. We further developed an iterative algorithm based on SCA to solve the formulated problem. The simulations have shown that the UAV battery capacity and the weighting factor have significant impact on the C&S performance.

## 7. ACKNOWLEDGEMENT

This paper has received funding from .....

## 8. REFERENCES

- [1] A. Liu, Z. Huang, M. Li, Y. Wan, W. Li, T. Han, et al, “A survey on fundamental limits of integrated sens-

- ing and communication,” *IEEE Commun. Surveys Tuts.*, Apr. 2021.
- [2] Y. Cui, F. Liu, X. Jing and J. Mu, “Integrating sensing and communications for ubiquitous IoT: Applications, trends, and challenges,” *IEEE Network*, vol. 35, no. 5, pp. 158-167, Oct. 2021.
- [3] F. Liu, Y. Cui, C. Masouros, J. Xu, T. Han, Y. Eldar, *et al*, “Integrated sensing and communications: Towards dual-functional wireless networks for 6G and beyond,” *IEEE J. Sel. Areas Commun.*, vol. 40, no. 6, pp. 1728-1767, June 2022.
- [4] X. Wang, Z. Fei, J. A. Zhang, J. Huang and J. Yuan, “Constrained utility maximization in dual-functional radar-communication multi-UAV networks,” *IEEE Trans. Commun.*, vol. 69, no. 4, pp. 2660-2672, April 2021.
- [5] Y. Zeng, R. Zhang, and T. J. Lim, “Wireless communications with unmanned aerial vehicles: Opportunities and challenges,” *IEEE Commun. Mag.*, vol. 54, no. 5, pp. 36-42, May, 2016.
- [6] Q. Wu, J. Xu, Y. Zeng, D. W. K. Ng, N. A. Dahir, R. Schober, and A. L. Swindlehurst, “A comprehensive overview on 5G-and-beyond networks with UAVs: From communications to sensing and intelligence,” *IEEE J. Sel. Commun.*, vol. 39, no. 10, pp. 2912-2945, Oct. 2021.
- [7] K. Meng, Q. Wu, S. Ma, W. Chen and T. Q. S. Quek, “UAV trajectory and beamforming optimization for integrated periodic sensing and communication,” *IEEE Wireless Commun. Lett.*, vol. 11, no. 6, pp. 1211-1215, June 2022.
- [8] Z. Lyu, G. Zhu, and J. Xu, “Joint maneuver and beamforming design for UAV-enabled integrated sensing and communication,” 2021, arXiv:2110.02857.
- [9] Y. Zeng, J. Xu, and R. Zhang, “Energy minimization for wireless communication with rotary-wing UAV,” *IEEE Trans. Wireless Commun.*, vol. 18, no. 4, pp. 2329 - 2345, Apr. 2019.
- [10] X. Jing, F. Liu, C. Masouros, and Y. Zeng, “ISAC from the sky: UAV trajectory design for joint communication and target localization,” arXiv preprint arXiv:2207.02904, 2022.
- [11] F. Liu, W. Yuan, C. Masouros and J. Yuan, “Radar-assisted predictive beamforming for vehicular links: communication served by sensing,” *IEEE Trans. Wireless Commun.*, vol. 19, no. 11, pp. 7704-7719, Nov. 2020.
- [12] Steven M. Kay, *Fundamentals of statistical signal processing: Estimation theory*. Upper Saddle River, U.S.: Prentice Hall, 1993, pp. 15-67.
- [13] Steven.M.Key, *Fundamentals of statistical signal processing, volume II: Detection theory*. Upper Saddle River, U.S.: Prentice Hall PTR, 1993, pp. 20-36.
- [14] S. Boyd and L. Vandenberghe, *Convex optimization*. Cambridge, U.K.: Cambridge Univ. Press, 2004.